

Synthesis and Olefin Polymerization Catalysis of New Divalent Samarium Complexes with Bridging Bis(cyclopentadienyl) Ligands

Eiji Ihara,[†] Mitsufumi Nodono,[†] Kenji Katsura,[†] Yoshifumi Adachi,[†]
Hajime Yasuda,^{*,†} Mizue Yamagashira,[‡] Hiroshi Hashimoto,[‡]
Nobuko Kanehisa,[‡] and Yasushi Kai^{*,‡}

Department of Applied Chemistry, Faculty of Engineering, Hiroshima University,
Higashi-Hiroshima 739-8527, Japan, and Department of Applied Chemistry,
Faculty of Engineering, Osaka University, Suita 565-0871, Japan

Received December 15, 1997

This paper deals with the preparation and olefin polymerization catalysis of six new divalent samarium complexes. These bridged bis(cyclopentadienyl) (Cp) complexes exhibit various structures with regard to the bridging group and the position of substituents on the Cp rings: *rac*-tBu, Me₂Si(2-Me₃Si-4-tBuC₅H₂)₂Sm(THF)₂ (**7**); *rac*-tBuMe₂Si, Me₂Si(2-Me₃Si-4-tBuMe₂SiC₅H₂)₂Sm(THF)₃ (**8**); C₁ symmetric, Me₂Si[2,4-(Me₃Si)₂C₅H₂][3,4-(Me₃Si)₂C₅H₂]-Sm(THF)₂ (**9**); *meso*, [1,2-(Me₂Si)(Me₂SiOSiMe₂)](3-tBuC₅H₂)₂Sm(THF)₂ (**10**); C_{2v} symmetric (Ph₂Si), Ph₂Si[3,4-(Me₃Si)₂C₅H₂]₂Sm(THF)₂ (**11**); C_{2v} symmetric [(SiOSi)₂], [1,2-(Me₂-SiOSiMe₂)₂](3-tBuC₅H₂)₂Sm(THF)₂ (**12**). The structures of **7**, **8**, **10**, and **12** were confirmed by X-ray crystallographic analysis. Among these divalent complexes, *meso* type complex **10** showed the highest activity for polymerizations of ethylene (5 × 10⁵ g of PE/(mol h)) and C₁-symmetric **9** afforded the highest molecular weight of polyethylene (M_n = 145 × 10⁴). Only racemic complexes **7** and **8** could polymerize 1-olefins such as 1-pentene and 1-hexene, giving highly isotactic polymers. Moreover, *rac*-**7** induces catalytic cyclopolymerization of 1,5-hexadiene to give poly(methylene-1,3-cyclopentane).

Introduction

Rare-earth-metal complexes have attracted much attention because of their unique reactivity as polymerization initiators.¹ Living polymerization of methyl methacrylate (MMA) was first achieved by the unique catalytic function of trivalent rare-earth-metal complexes with two pentamethylcyclopentadienyl ligands, Cp*₂SmR, affording highly syndiotactic poly(MMA) quantitatively in a short period.² Furthermore, the bis-Cp*-based rare-earth-metal complexes promote the living polymerization of alkyl acrylate (methyl acrylate, ethyl acrylate, and butyl acrylate),³ which is very difficult to attain by conventional catalysts because of the presence of acidic protons in the main chain. Four-, six-, and seven-membered lactones can also be polymerized in a living manner by these complexes.⁴

Furthermore, rare-earth-metal complexes are very effective for polymerization of nonpolar monomers such as ethylene and 1-olefins.⁵ The greatest advantage of rare-earth-metal catalysts lies in high polymerization

catalytic activity toward olefins even in the absence of "methylaluminoxane". Bis(pentamethylcyclopentadienyl) (Cp*) rare-earth-metal hydrides, LnH(C₅Me₅)₂ (Ln = La, Nd, Sm), have been reported to be quite active for ethylene polymerization, although these are completely inactive for the 1-olefin polymerization.^{5c} Recently, modified Cp-based complexes such as [(C₅Me₄-SiMe₂(η-NCMe₃)Sc(η-H))₂],⁶ [*rac*-Me₂Si(2-SiMe₃-4-CMe₃-C₅H₂)₂YH]₂,⁷ and the mixed Cp*-alkoxide complex [Y(C₅Me₅)(OC₆H₃-2,6-tBu₂)(η-H)]₂⁸ have been reported to be active for the polymerizations of 1-olefins. The reactivity of the latter complexes suggests that the synthesis of high-molecular-weight polyethylene can be achieved by the appropriate substitution of Cp ligand in rare-earth-metal complexes.

Divalent samarium complexes also catalyze ethylene polymerization as trivalent complexes do as noted above.⁹ Although bis-Cp* complexes such as Cp*₂Sm and Cp*₂Sm(THF)₂ show high polymerization activity toward ethylene, molecular weights of the resulting

[†] Hiroshima University.

[‡] Osaka University.

(1) (a) Yasuda, H.; Tamai, H. *Prog. Polym. Sci.* **1993**, *18*, 1097. (b) Yasuda, H.; Ihara, E. *Adv. Polym. Sci.* **1997**, *133*, 53.

(2) (a) Yasuda, H.; Yamamoto, H.; Yamashita, M.; Yokota, K.; Nakamura, A.; Miyake, S.; Kai, Y.; Kanehisa, N. *Macromolecules* **1993**, *26*, 7134. (b) Yasuda, H.; Yamamoto, H.; Yokota, K.; Miyake, S.; Nakamura, A. *J. Am. Chem. Soc.* **1992**, *114*, 4908.

(3) Ihara, E.; Morimoto, M.; Yasuda, H. *Macromolecules* **1995**, *28*, 7886.

(4) Yamashita, M.; Takemoto, Y.; Ihara, E.; Yasuda, H. *Macromolecules* **1996**, *29*, 1798.

(5) (a) Watson, P. L.; Parshall, G. W. *Acc. Chem. Res.* **1985**, *18*, 51. (b) Burger, B. J.; Thompson, M. E.; Cotter, W. D.; Bercaw, J. E. *J. Am. Chem. Soc.* **1990**, *112*, 1566. (c) Yang, X.; Stern, C. L.; Marks, T. J. *Organometallics* **1991**, *10*, 840.

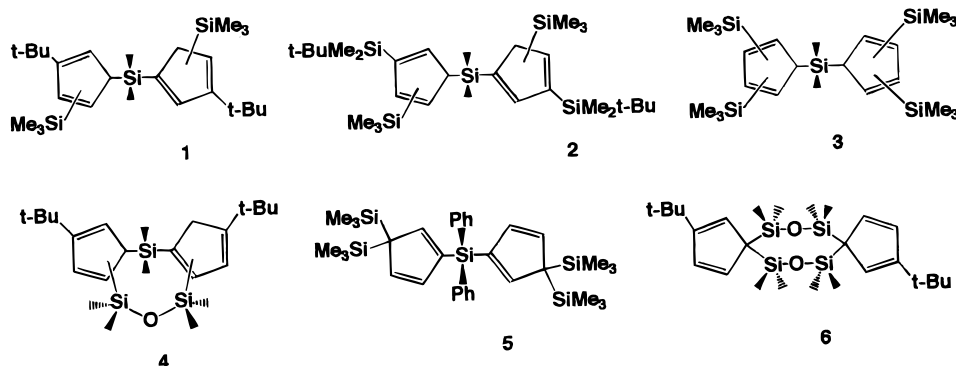
(6) Coughlin, E. B.; Bercaw, J. E. *J. Am. Chem. Soc.* **1992**, *114*, 7606.

(7) (a) Coughlin, E. B.; Shapiro, P. J.; Bercaw, J. E. *Polym. Prepr., Am. Chem. Soc. Div. Polym. Chem.* **1992**, *33*, 1266. (b) Shapiro, P. J.; Cotter, W. D.; Schaefer, W. P.; Labinger, J. A.; Bercaw, J. E. *J. Am. Chem. Soc.* **1994**, *116*, 4623.

(8) Schaverien, C. J. *Organometallics* **1994**, *13*, 69.

(9) (a) Watson, P. L.; Herskovitz, T. *ACS Symp. Ser.* **1983**, No. 212, 459. (b) Evans, W. J.; Ulibarri, T. A.; Ziller, J. W. *J. Am. Chem. Soc.* **1990**, *112*, 2314.

Chart 1



polymers are rather low ($M_n < 25\,000$). Furthermore, Cp^*_2Sm reacts with various 1-olefins to give stable π -allyl complexes and lacks the activity for polymerization of 1-olefins.^{9b} Judging from the result of the divalent complexes, there may be a great possibility of improving the catalytic action toward olefin polymerization by modification of the ligand environment with bulky substituents. Herein, we describe the preparation of six new divalent samarium complexes bearing various substituted bis-Cp ligands and the result of ethylene and 1-olefin polymerizations.

Results and Discussion

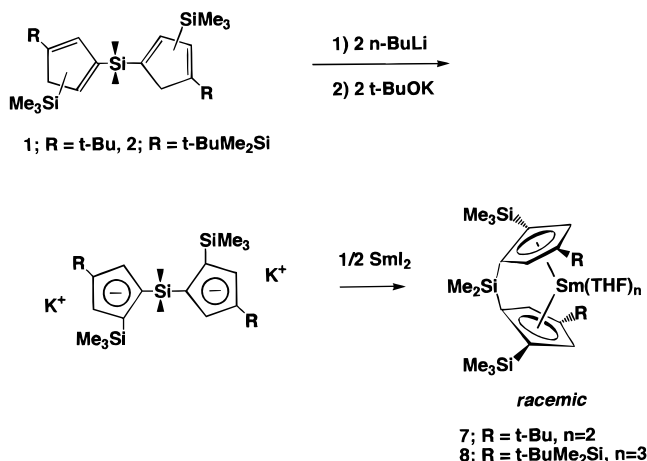
Ligand Synthesis. To investigate the relationship between the structure of the initiator and its polymerization activity, we first synthesized a series of ligands which afforded various type of rare-earth-metal complexes. Six ligands used in this study are summarized in Chart 1 (preparation methods are given in the Supporting Information). All the reactions proceed smoothly to afford the desired complexes in good yield.

During the preparation of these complexes, the following points became apparent. (1) *t*-Bu and *t*-BuMe₂Si substituents can be fixed at the 3- and 4-positions in bridging Cp ligands **1** and **2**. (2) The positions of C–C double bonds and Me₃Si groups in the Cp ring cannot be fixed in the case of **1**–**4**. Therefore, we could not determine the precise structures of **1**–**4** by the NMR method because of the existence of various isomers. However, a single samarium complex was formed when these were complexed with Sm (*vide infra*).

On the other hand, we can easily characterize the structure of **5** by the analysis of its ¹H NMR spectrum. Since three correlated signals of protons on Cp rings are observed in an ABX pattern, it is apparent that these protons are connected to an sp² carbon on the five-membered ring. Accordingly, two Me₃Si groups are on the same sp³ carbon at 3-positions as shown in the formula. However, when this ligand was reacted with the appropriate rare-earth-metal, a (3,4-bis(trimethylsilyl)cyclopentadienyl)metal compound was obtained as a result of sigmatropic rearrangement.¹⁰

Synthesis of Sm(II) Complexes. All the divalent samarium complexes were synthesized by the reaction of the dipotassium salt of the corresponding ligand with

Scheme 1



SmI_2 . Since the Me₃Si or Me₂Si group in the Cp ligand is very sensitive to KH, potassium salts of the ligands were prepared by lithiation with *n*-BuLi followed by cation exchange reaction with *t*-BuOK.

(a) Racemic Complexes 7 and 8. The reaction of dipotassium salt of **1** with SmI_2 afforded Me₂Si(2-Me₃Si-4-*t*-BuC₅H₂)₂Sm(THF)₂ (**7**) (*rac*-*t*-Bu), as purple crystals (Scheme 1). The ¹H NMR spectrum of **7** shows each *t*-Bu, Me₃Si, and bridging Me₂Si signal as one singlet, suggesting that **7** has a C₂-symmetric structure. The integral ratio of the NMR spectrum shows the presence of two THF molecules coordinated to the Sm center. Single-crystal X-ray analysis clearly reveals the racemic structure (Figure 1). Crystal data for complexes **7**, **8**, **10**, and **12** are given in Table 1 and selected bond lengths and angles in Table 2. Each *t*-Bu and Me₃Si group is located on the 2- and 4-positions, respectively, on both Cp rings, and the C₂-symmetric structure was formed. The arrangement of the substituents is just the same as that of the trivalent Y complex *rac*-Me₂Si(2-Me₃Si-4-*t*-BuC₅H₂)₂YCl₂Li(THF)₂, reported by Bercaw et al.⁷ The Cp'(centroid)–Sm–Cp'(centroid) bite angle is 115.8(4)°, ca. 20° smaller than that of (C₅Me₅)₂Sm(THF)₂ bearing no Me₂Si bridge.¹¹ The decrease of the bite angle corresponds to the increase of the space around the metal center, from which we can expect high catalytic reactivity for olefin monomers.¹²

In a similar manner, *rac*-Me₂Si(2-Me₃Si-4-*t*-BuMe₂SiC₅H₂)₂Sm(THF)₃ (**8**) (*rac*-*t*-BuMe₂Si) was synthesized

(10) (a) Jutzi, P. *Chem. Rev.* **1986**, *86*, 983. (b) Ustynyuk, Yu. A.; Kisin, A. V.; Pribytkova, J. M.; Zarkin, A. A.; Antonova, N. D. *J. Organomet. Chem.* **1972**, *42*, 47. (c) Grishin, Yu. K.; Luzikov, Yu. N.; Ustynyuk, Yu. A. *Dokl. Acad. Nauk SSSR* **1974**, *216*, 321.

(11) Evans, W. J.; Grate, J. W.; Choi, H. W.; Bloom, I.; Hunter, W. E.; Atwood, J. L. *J. Am. Chem. Soc.* **1985**, *107*, 941.

(12) Jeske, G.; Schock, L. E.; Swepston, P. N.; Schumann, H.; Marks, T. J. *J. Am. Chem. Soc.* **1985**, *107*, 8103.

Table 1. Crystal Data for 7, 8, 10, and 12

	7	8	10	12
formula	C ₃₄ H ₆₂ O ₂ SmSi ₃	C ₄₂ H ₈₂ O ₃ SmSi ₅	C ₃₂ H ₅₆ O ₃ SmSi ₃	C ₃₄ H ₆₂ O ₄ SmSi ₄
fw	737.52	925.94	1171.55	797.60
cryst syst	monoclinic	monoclinic	orthorhombic	orthorhombic
space group	<i>Cc</i>	<i>P2₁/c</i>	<i>Pbca</i>	<i>P2₁2₁2₁</i>
<i>a</i> /Å	12.309(2)	12.147(3)	19.386(6)	17.316(5)
<i>b</i> /Å	17.153(2)	20.780(3)	25.251(4)	20.093(4)
<i>c</i> /Å	19.496(3)	21.718(2)	17.386(4)	11.761(4)
β /deg	103.45(1)	103.55(1)		
<i>V</i> /Å ³	4003(1)	5329(1)	8510(3)	4092(1)
<i>Z</i>	4	4	8	4
<i>D</i> _{calcd} /(g cm ⁻³)	1.224	1.154	1.129	1.295
<i>F</i> (000)	1544	1964	3008	1664
μ (Mo K α)/cm ⁻¹	15.84	12.47	14.91	15.87
no. of measd rflns	4986	10172	10648	5236
no. of obsd rflns (<i>F</i> _o \geq 3.0 σ (<i>F</i> _o))	3110	3540	3556	4117
<i>R</i> ^a (<i>R</i> _w) ^b	0.076 (0.048)	0.082 (0.074)	0.079	0.057 (0.066)

^a $R = \sum ||F_o| - |F_c|| / \sum |F_o|$. ^b $R_w = (\sum w(|F_o| - |F_c|)^2 / \sum w|F_o|^2)^{1/2}$; $w = 1/\sigma^2(F_o)$.

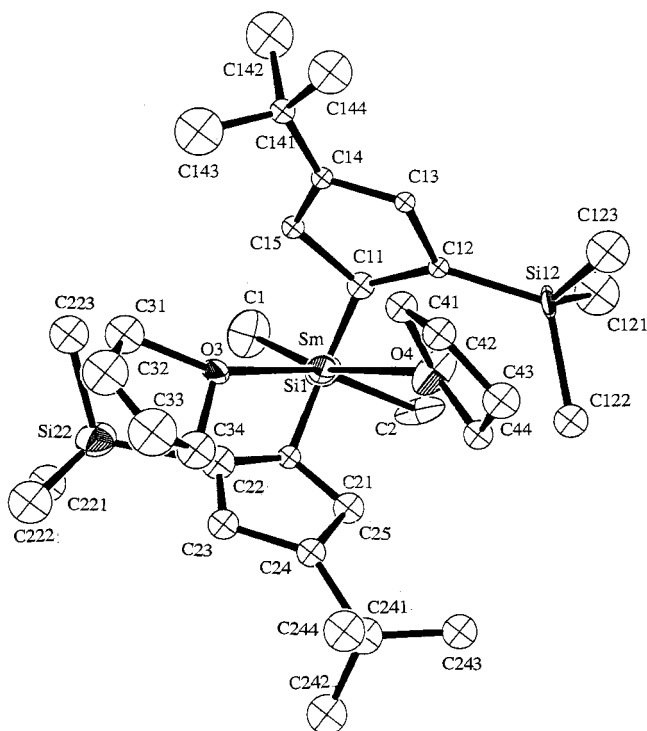


Figure 1. Structure of racemic-tBu 7.

by the path shown in Scheme 1. The ¹H NMR spectrum of **8** reveals *C*₂-symmetric features, in which tBu, Me₃-Si, and Me₂Si groups appear as singlets. Two diastereotopic Me signals for tBuMe₂Si indicate the presence of a chiral center. Supporting the result of ¹H NMR, X-ray analysis reveals the racemic structure of **8** (Figure 2). The formation of a racemic complex from **2** is in good accord with the data for a trivalent Y complex with this ligand, Me₂Si(2-Me₃Si-4-tBuMe₂SiC₅H₂)₂YCl₂Li(THF)₂.¹³ The Cp'(centroid)-Sm-Cp'(centroid) bite angle is 116.5°, again 20° smaller than that of the nonbridged bis-Cp complex Cp*₂Sm(THF)₂.

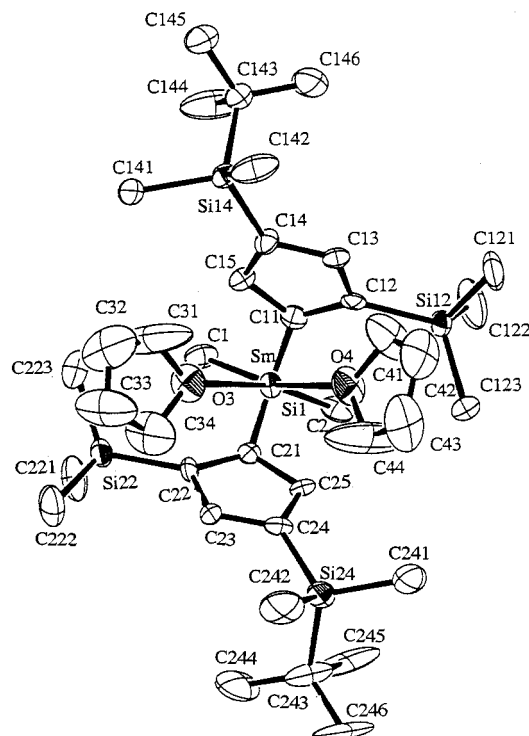
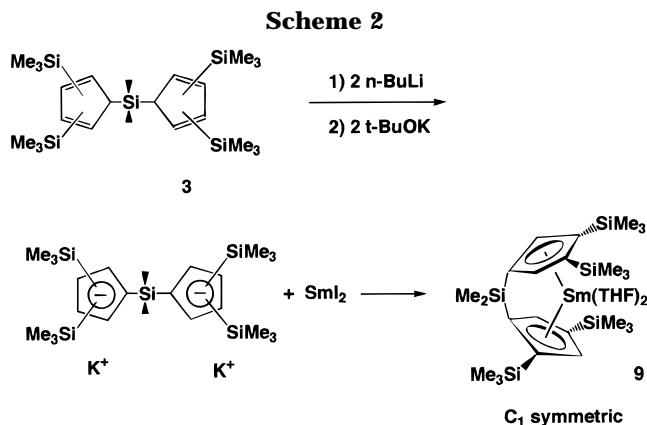
The remarkable difference observed between **7** and **8** is the number of THF molecules coordinated to the complexes (2 in **7**, 3 in **8**). Though one of the THF molecules in **8** does not coordinate in the X-ray structure, all three THF molecules appear equivalently in ¹H NMR, indicating the existence of rapid exchange

Table 2. Selected Bond Lengths (Å) and Angles (deg)

	7	8	10	12
Bond Lengths				
C(11)-C(12)	1.58(4)	1.55(4)	1.42(4)	1.42(2)
C(12)-C(13)	1.55(2)	1.45(4)	1.46(4)	1.42(2)
C(13)-C(14)	1.40(3)	1.43(4)	1.39(4)	1.42(2)
C(14)-C(15)	1.28(3)	1.48(5)	1.43(4)	1.39(2)
C(15)-C(11)	1.59(4)	1.45(4)	1.42(4)	1.42(2)
C(21)-C(22)	1.28(4)	1.42(4)	1.40(4)	1.42(2)
C(22)-C(23)	1.25(3)	1.43(4)	1.42(4)	1.43(2)
C(23)-C(24)	1.45(3)	1.38(5)	1.40(4)	1.41(2)
C(24)-C(25)	1.59(4)	1.42(4)	1.41(4)	1.40(2)
C(25)-C(21)	1.27(4)	1.41(4)	1.43(4)	1.41(2)
Si(1)-C(1)	1.73(5)	1.87(4)	1.86(3)	
Si(1)-C(2)	1.98(4)	1.90(3)	1.85(4)	
Sm-O(3)	2.61(2)	2.58(3)	2.54(2)	2.669(9)
Sm-O(4)	2.67(2)	2.63(3)	2.56(2)	2.591(9)
C(12)-Si(12)	1.80(2)			
C(22)-Si(22)	1.93(4)			
C(14)-Si(14)		1.88(3)		
C(24)-Si(24)		1.91(3)		
C(12)-Si(2)			1.85(2)	
C(22)-Si(3)			1.89(3)	
C(11)-Si(2)				1.88(1)
C(12)-Si(4)				1.87(1)
C(21)-Si(3)				1.85(1)
C(22)-Si(5)				1.84(1)
Bond Angles				
O(3)-Sm-O(4)	80.2(7)	77.8(10)	94.4(8)	99.6(3)
Si(2)-O(1)-Si(3)			142(1)	147.2(7)
Si(2)-O(2)-Si(5)				142.8(7)
Cp(centroid)-Sm-Cp(centroid)	115.8	116.5	116.5	133.4
Cp'-Cp'	78.2	77.3	76.0	55.4

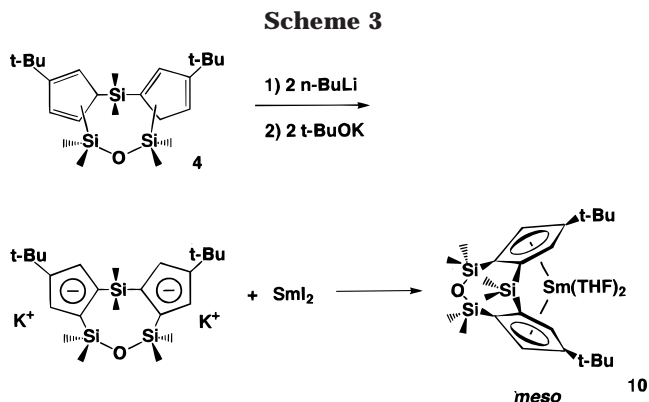
among these molecules. Furthermore, two of the THF molecules can be removed by repeated washing with toluene or heating. This procedure is especially important to obtain a higher activity of **8** toward olefin polymerization.

The dihedral angle between the planes containing Cp'(centroid)-Sm-Cp'(centroid) and O(THF)-Sm-O(THF) is 72.7° for **7** and 76.4° for **8**, respectively. Comparing these data with those of other divalent complexes, 86.2° for Cp*₂Sm(THF)₂, 89.4° for **10**, and 88.2° for **12**, the deviation of the dihedral angle from 90° is concluded to be a characteristic structural feature of the racemic complexes. In these racemic complexes, oxygen atoms of THF molecules cannot exist in the equatorial plane defined by two Cp rings because of the presence of bulky substituents at the 4-position on the Cp ring. As will be described later in this paper, only these racemic complexes showed high activities toward

**Figure 2.** Structure of *racemic*-tBuMe₂Si **8**.

the polymerization of 1-olefins. Thus, the reactivity to 1-olefins may be closely related to the structural perturbation caused by the bulky substituents.

(b) *C*₁-Symmetric Complexes **9.** The *C*₁-symmetric Sm(II) complex Me₂Si[2,4-(Me₃Si)₂C₅H₂][3,4-(Me₃Si)₂-C₅H₂][Sm(THF)₂] (**9**), in which two Me₃Si groups are located at 3,4-positions in one Cp ring and at 2,4-positions in another ring, was prepared by the reaction of dipotassium salt **3** with SmI₂ in THF (Scheme 2). The ¹H NMR spectrum of **9** is shown in Figure 3. Each signal of four Me₃Si and four Cp H groups and two bridging Me₂Si groups appears separately. In the synthesis of trivalent Sm complexes with this ligand, we obtained a mixture of racemic and *C*₁-symmetric complexes and confirmed their structures by ¹H NMR and X-ray analysis.¹⁴ Whereas the ¹H NMR spectrum of this tris racemic complex showed highly symmetrical features (two Me₃Si, two Cp H, and one bridging Me₂Si signal) much the same as those of **7**, four Me₃Si, four Cp H, and two bridging Me₂Si signals appeared in the spectrum in the case of the trivalent *C*₁-symmetric complex. Thus, the NMR spectrum of **9** resembles that



of the *C*₁-symmetric samarium(III) species, in which two Me₃Si groups are at 2,4-positions in one Cp and at 3,4-positions in the other Cp.

It should be noted that the divalent *C*₁-symmetric complex was formed exclusively, presumably due to the large steric bulk of two coordinated THF molecules, whereas a mixture of racemic and *C*₁-symmetric complexes was obtained in the case of trivalent complexes because of the reduced steric bulk.¹⁴

(c) *meso* Type Complexes **10.** The ligand **4**, which has two bridging groups of different length (–Me₂Si–, –Me₂SiOMe₂Si–), was designed to afford a *meso* type structure after complexation (Scheme 3). The ¹H NMR spectrum of the complex obtained by the reaction of the potassium salt of **4** with SmI₂ shows each bridging group (Me₂SiOSiMe₂, Me₂Si) as two singlets and tBu groups as one singlet, indicating that this complex has *C*_s symmetry. On the basis of X-ray structure analysis, we finally confirmed the *meso* type structure for **10** (Figure 4). Despite the presence of an additional bridging group (Me₂SiOSiMe₂), the Cp(centroid)–Sm–Cp(centroid) bite angle is 116.5°, which is very close to that of **7** and **8** bearing one Me₂Si bridge. Thus, the presence of the additional SiOSi bridge did not affect the bite angle.

The O(3)–Sm–O(4) angle is 94.4°, which is about 15° larger than those of **7** and **8**. Whereas the C(α)–O–C(α) plane of one THF molecule is nearly parallel to the equatorial plane defined by Sm, O(3), and O(4) (dihedral angle 2.5°), the plane of the other THF is nearly perpendicular to this plane (dihedral angle 89.2°). This orientation of the latter THF molecule allows the oxygen to form a π-bond with Sm. Though the coordination mode of these two THF molecules is energetically the most stable, other divalent Sm complexes including

(14) A mixture of the racemic and *C*₁-symmetric trivalent Sm complexes was obtained by the reaction of the dilithium salt of **3** with SmCl₃, and they were separated by using their different solubilities in hexane. Full details about these trivalent complexes will be reported elsewhere. Racemic Me₂Si[2,4-(SiMe₃)₂C₅H₂]₂SmCl₂Li(THF)₂: ¹H NMR (400 MHz, C₆D₆) δ –1.73 (s, 18H, SiMe₃), 0.01 (s, 18H, SiMe₃), 2.01 (s, 8H, THF-β), 2.27 (s, 6H, Me₂Si), 4.76 (s, 8H, THF-α), 5.84 (s, 2H, Cp H), 16.37 (s, 2H, Cp-H); cell data triclinic, *P*1 (No. 2), *a* = 12.611(4) Å, *b* = 17.109(3) Å, *c* = 12.134(4) Å, α = 99.74(3)°, β = 115.16(2)°, γ = 90.91(3)°, *D*_{calc}(*Z* = 2) = 1.211 g/cm³. Least-squares refinement based on 4239 reflections converged to *R* = 0.115 and *R*_w = 0.128. *C*₁-symmetric Me₂Si[2,4-(SiMe₃)₂C₅H₂][3,4-(SiMe₃)₂C₅H₂][SmCl₂Li(THF)₂]: ¹H NMR (400 MHz, C₆D₆) δ –2.33 (s, 9H, SiMe₃), –0.82 (s, 9H, SiMe₃), –0.54 (s, 9H, SiMe₃), 1.14 (s, 3H, Me₂Si), 1.18 (s, 9H, SiMe₃), 1.85 (s, 8H, THF-β), 2.97 (s, 3H, Me₂Si), 4.01 (s, 1H, Cp H), 4.43 (s, 8H, THF-α), 9.73 (s, 1H, Cp H), 10.35 (s, 1H, Cp H), 17.10 (s, 1H, Cp H); cell data monoclinic, *P*2₁/c (No. 14), *a* = 17.483(3) Å, *b* = 13.427(3) Å, *c* = 19.475(2) Å, β = 104.23(1)°, *D*_{calc}(*Z* = 4) = 1.270 g/cm³. Least-squares refinement based on 3851 reflections converged to *R* = 0.068 and *R*_w = 0.049.

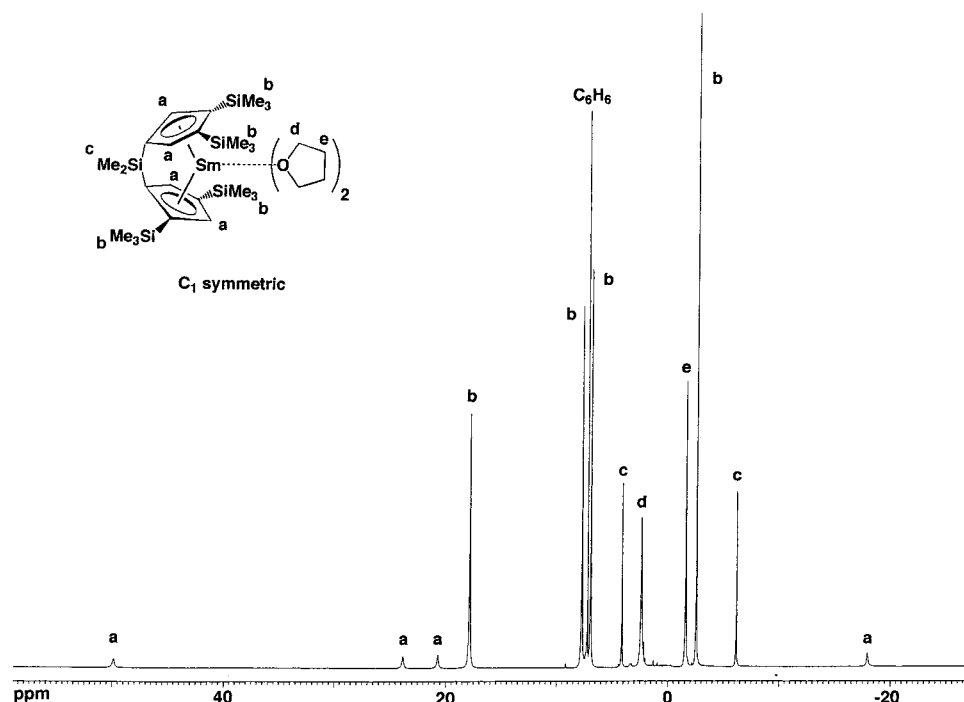


Figure 3. ^1H NMR spectrum of C_1 -symmetric **9**.

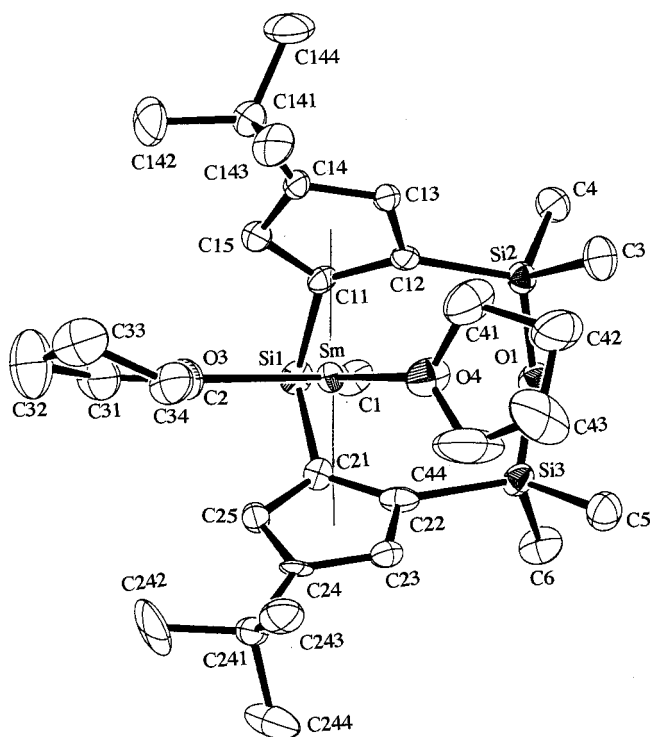
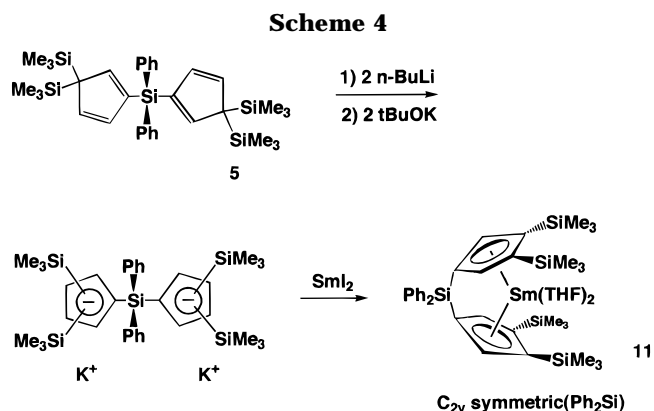


Figure 4. Structure of *meso* **10**.

$\text{Cp}^*_2\text{Sm}(\text{THF})_2$ cannot produce such a stable structure because of the severe steric repulsion between THF and Me substituents on Cp rings. As will be discussed later in this paper, such a difference of the initiator structure is reflected on the reactivity for olefins.

(d) C_{2v} -Symmetric (Ph_2Si) Complex **11.** In the ligand **5**, a Ph_2Si bridge was used in place of Me_2Si , to investigate the effect of a bulky bridging group on the structure of the resulting complex. In the complexation with a trivalent Sm metal, **5** afforded the C_1 -symmetric complex exclusively, whereas a mixture of racemic and C_1 -symmetric complexes was obtained from **3**, bearing



a Me_2Si bridge.¹⁵ The steric repulsion of the Ph group with the Me_3Si group at the 2-position of the Cp ring will prevent the formation of racemic complex in the case of the trivalent complexes.

The complexation of dipotassium salt of **5** with SmI_2 gave the divalent complex **11** as purple crystals (Scheme 4). The ^1H NMR spectrum of complex **11** (Figure 5) shows only one signal for Me_3Si groups and Cp H protons, respectively. Therefore, we can readily conclude that **11** has a highly symmetrical structure, a C_{2v} -symmetric structure where all four Me_3Si groups are at 3,4-positions of both Cp rings. The structure in which two Me_3Si groups are located at 2,5- or 2,4-positions can be neglected for steric reasons.

Comparing the result of the complexation of divalent samarium complexes (C_1 from **3**, C_{2v} from **5**) and trivalent complexes (C_1 and racemic from **3**, C_1 from **5**), we can conclude that the arrangement of two Me_3Si groups at 3- and 4-positions on the Cp ring will be more

(15) Cell data for C_1 -symmetric $\text{Ph}_2\text{Si}[2,4-(\text{SiMe}_3)_2\text{C}_5\text{H}_2][3,4-(\text{SiMe}_3)_2\text{C}_5\text{H}_2]\text{SmCl}_2\text{Li}(\text{THF})_2$: triclinic, $P1$ (No. 2), $a = 14.557(2)$ Å, $b = 15.145(2)$ Å, $c = 13.184(2)$ Å, $\alpha = 104.47(1)^\circ$, $\beta = 92.99(1)^\circ$, $\gamma = 83.17(1)^\circ$, $D_{\text{calc}}(Z = 2) = 1.155$ g/cm³. Least-squares refinement based on 8814 reflections converged to $R = 0.058$ and $R_w = 0.072$.

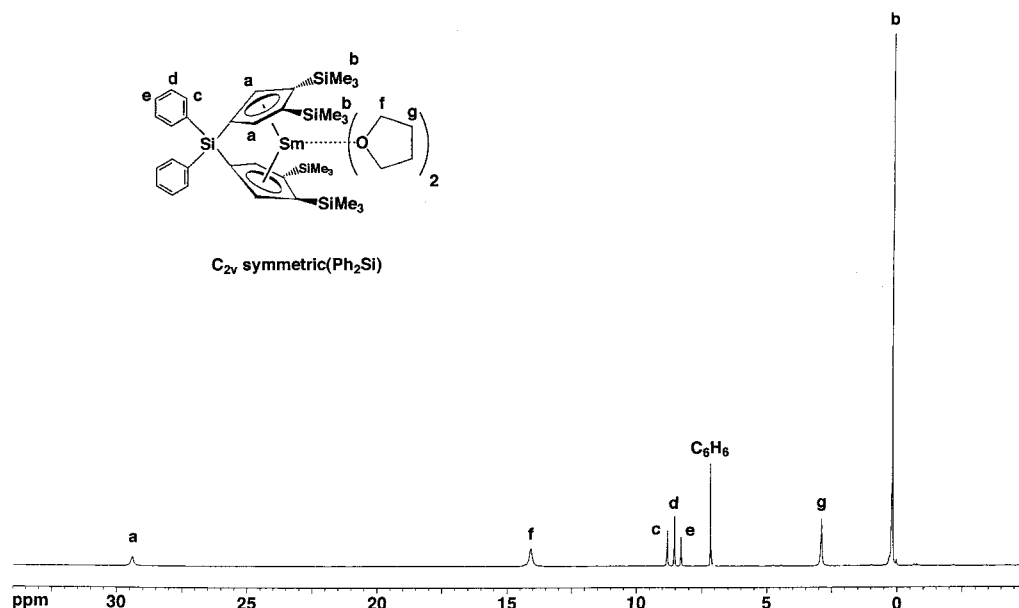
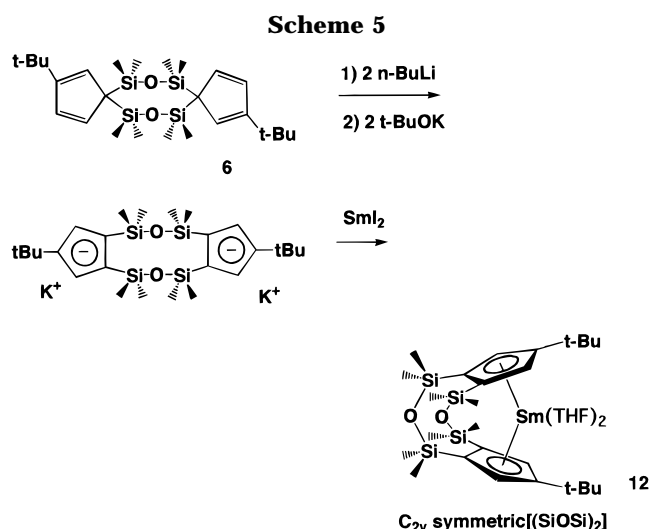


Figure 5. ^1H NMR spectrum of C_{2v} -symmetric (Ph_2Si) **11**.



favorable in the case of divalent complexes. This may arise from the different mode of coordination to the metal (steric bulk of Sm center: $\text{L}_2\text{M}[\text{THF}]_2 > \text{L}_2\text{MCl}_2\text{Li}[\text{THF}]_2$) and/or the different electronic natures of di- and trivalent Sm metals.

(e) C_{2v} -Symmetric $[(\text{SiOSi})_2]$ Complex **12.** The ligand **6** with two $\text{Me}_2\text{SiOSiMe}_2$ bridging groups also afforded a C_{2v} -symmetric structure after complexation with divalent samarium complexes (Scheme 5). Its structure was characterized by ^1H NMR and finally by X-ray structure analysis (Figure 6). One t-Bu, one Cp-H, and two $\text{Me}_2\text{SiOSiMe}_2$ signals appear as singlets in ^1H NMR, indicating a C_{2v} -symmetric structure for **12**. Cp'(centroid)–Sm distances are 2.64 and 2.63 Å, which are similar to those of the other complexes studied here. The Cp'(centroid)–Sm–Cp'(centroid) bite angle (133.4°) is very close to that of $\text{Cp}^*_2\text{Sm}(\text{THF})_2$ (137°). Thus, the use of long bridging groups did not result in the elongation of the Cp'(centroid)–Sm distance but resulted in an increase in the Cp'(centroid)–Sm–Cp'(centroid) bite angle.

(f) Structural Perspective of the Divalent Sm Complexes. In Chart 2, the structures of all the

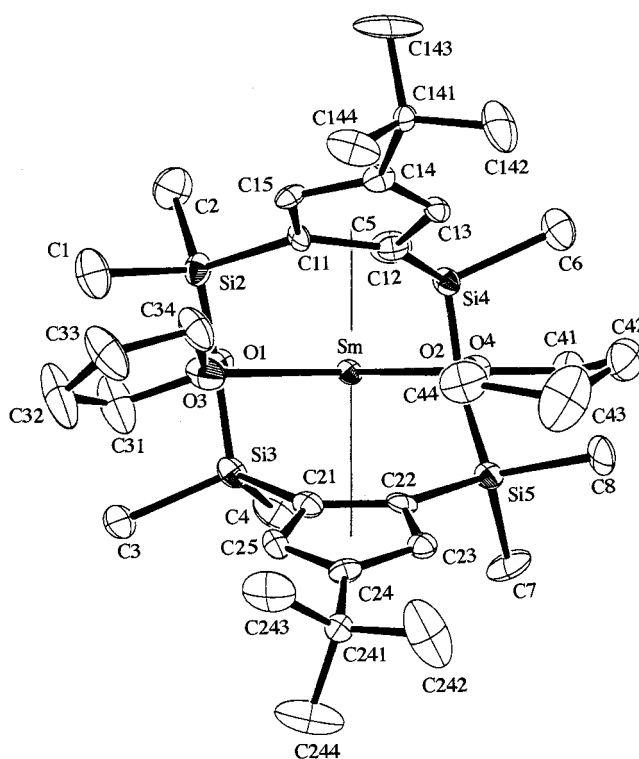


Figure 6. Structure of C_{2v} -symmetric $[(\text{SiOSi})_2]$ **12**.

divalent samarium complexes reported in this text are given schematically. The following points are obvious from the illustration.

(1) Each complex has an unique shape of the vacant space around the samarium center, when we consider neglecting the coordinated THF.

(2) In a series of Me_2Si -bridged complexes (**7**–**12**), the size of the vacant space around the metal center increases gradually in the order $C_{2v}(\text{Ph}_2\text{Si})$ **11** < $C_{2v}[(\text{SiOSi})_2]$ **12** < C_1 **9** < racemic **7** < *meso* **10** (the racemic **8** cannot be included in this order since the effect of the larger substituent, tBuMe₂Si, on the size of the space cannot be easily estimated). Thus, the movement of the substituent on the Cp ring resulted in an increase of

Chart 2

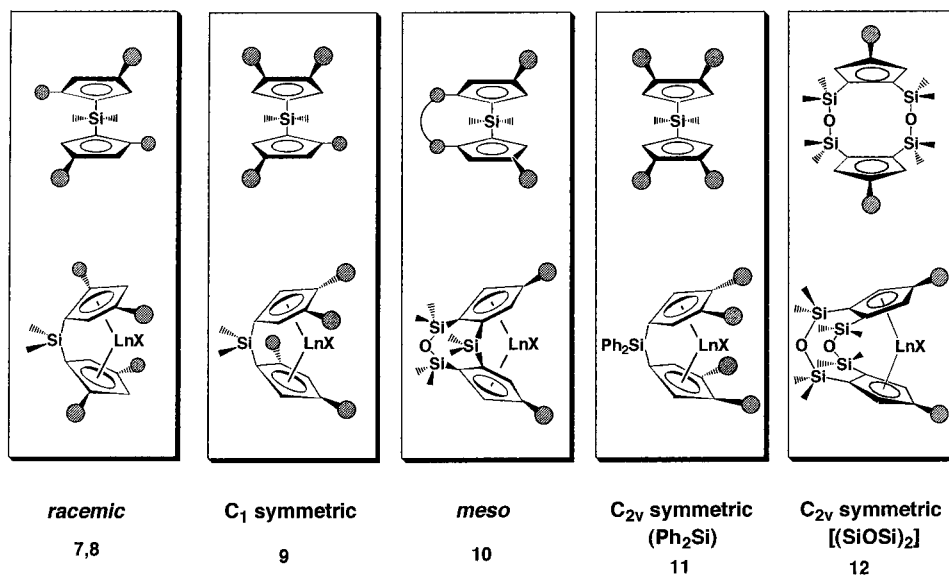
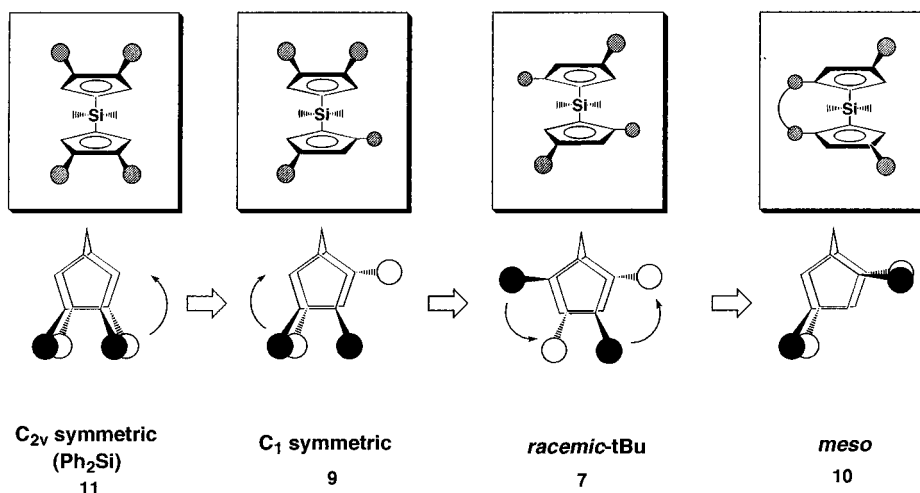


Chart 3



the vacant space around the metal center, as shown in Chart 3.

The effective volumes V_{eff} , the space around the metal atom for olefin coordination, were calculated using the SV program¹⁶ for complexes **7**, **8**, **10**, and **12**, respectively (calculation was carried out for the THF-free molecule) (Figure 7). The V_{eff} values in the complexes are in the order **8** \approx **7** \approx **10** $>$ **12**, indicating that the reactivity for olefin polymerization increases in this order. In fact, low catalytic activity for complex **12** is well-interpreted in terms of resulting effective volume. However, the accuracy of this calculation is not so high as to differentiate the effective volumes among **8**, **7**, and **10**.

Ethylene Polymerization. Ethylene polymerization was explored by using the resulting six divalent Sm complexes. Although the divalent samarium complex does not possess a carbon–metal bond into which ethylene can insert, it can polymerize the monomer effectively. Recently, Evans et al. have investigated the mechanism of ethylene polymerization by Cp^*_2Sm using

field desorption mass spectrometry (FD-MS).¹⁷ They proposed the polymerization mechanism as shown in Scheme 6. The initiation is the formation of a 2:1 complex of Cp^*_2Sm with ethylene followed by electron transfer, giving a trivalent alkyl complex with two $\text{Sm}-\text{C}$ bonds. In fact, the 2:1 complexes of Cp^*_2Sm with unsaturated compounds have been isolated and crystallographically characterized in the case of dinitrogen,¹⁷ azobenzene,¹⁹ styrene,²⁰ *trans*-stilbene,²⁰ and diphenylbutadiene.²¹ Then, the propagation is supposed to follow the successive insertion of ethylene into the $\text{Sm}-\text{C}$ bond, where the catalyst behaves as a bifunctional initiator. Thus, experimental results were consistent with the proposed mechanism. The polymerization under a D_2 atmosphere also resulted in the quantitative incorporation of deuterium atoms into both chain ends of ethylene

(17) Evans, W. J.; DeCoster, D. M.; Greaves, J. *Macromolecules* **1995**, *28*, 7929.

(18) Evans, W. J.; Ulibarri, T. A.; Ziller, J. W. *J. Am. Chem. Soc.* **1988**, *110*, 6877.

(19) Evans, W. J.; Drummond, D. K.; Bott, S. G.; Atwood, J. L. *Organometallics* **1986**, *5*, 2389.

(20) Evans, W. J.; Ulibarri, T. A.; Ziller, J. W. *J. Am. Chem. Soc.* **1990**, *112*, 219.

(21) Evans, W. J.; Keyer, R. A.; Ziller, J. W. *Organometallics*, **1993**, *12*, 2618.

(16) Nemoto, T.; Ohashi, Y. SV Program for Viewing Crystal and Molecular Structures; Tokyo Institute of Technology, Tokyo, Japan, 1993.

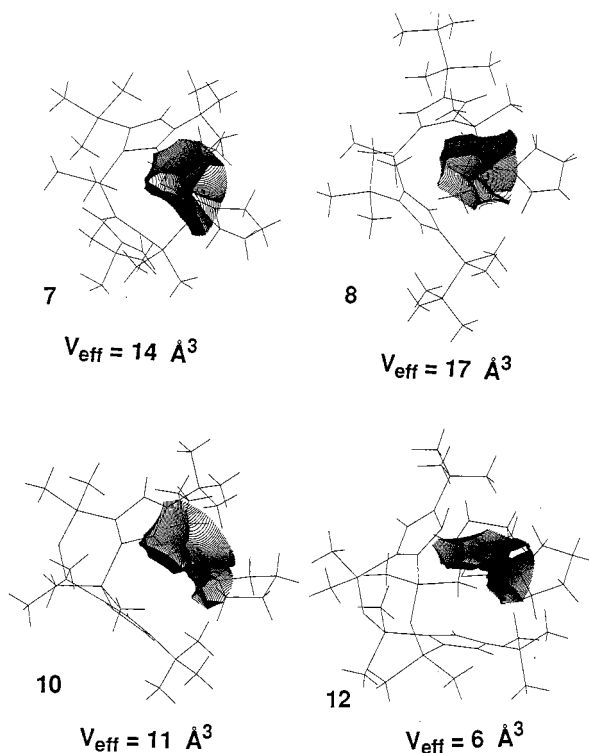


Figure 7. Effective volumes (V_{eff}) for monomer coordination to metal.

oligomers. Thus, we can readily estimate the initiation mechanism for complexes **7–12** as insertion of ethylene between two divalent complexes.¹⁷

Activity of the Complexes. The result of the ethylene polymerization is summarized in Table 3. In a series of the complexes with two (or one) coordinated THF molecules, the activity of the ethylene polymerization decreases in the order *meso* **10** > racemic **7** > C_{2v} -symmetric(Ph_2Si) **11** > racemic **8** > C_1 -symmetric **9** >> C_{2v} -symmetric($[\text{SiOSi}]_2$) **12**. The order of activity changes primarily depending upon the size of the vacant space around the Sm center. Thus, the *meso* complex **10** exhibited the highest activity due to the large space around the Sm center and the C_{2v} -symmetric($[\text{SiOSi}]_2$) **12** complex showed the lowest activity. The racemic complex with the $t\text{-BuMe}_2\text{Si}$ group **8** and the C_{2v} complex (Ph_2Si) **11** did not show polymerization activity at all when the complex is coordinated by two or three THF molecules. Inhibition of polymerization is mainly due to their large steric bulk, and removal of the

coordinated THF by heating or washing with toluene is required. From the results noted above, we can conclude the following.

(1) The activity of the ethylene polymerization by divalent Sm complexes varies depending upon how easy the incoming ethylene coordinates to the Sm atom. Thus, optimum space around the metal center is necessary for high activity (the optimum space not only is defined by vacant space around the metal but also is effected by the number of coordinated THF atoms and the steric environment derived from the substituents).

(2) The coordination of two or three THF molecules prevents the approach of ethylene to the Sm atom, and as a result only low activity was observed. When complete elimination of coordinated THF is realized, we will be able to determine the more detailed reaction mechanism.

(3) The initiation mechanism for **10**, **7**, and **9** is illustrated in Chart 4. The largest vacant site was observed in the case of **10** and the smallest one in the case of **9**. Thus, we can estimate the real vacant site by considering the complexation between one ethylene molecule and two lanthanide complexes.

Molecular Weight of Polyethylenes. As can be seen from Table 3, the *meso* type complex **10** with the highest activity gave the lowest molecular weight of the polymers ($M_n < 50\,000$). On the other hand, racemic and C_1 - and C_{2v} -symmetric complexes gave very high molecular weight polyethylenes ($M_n > 100\,000$). The molecular weight of polyethylene should vary depending upon how often the termination or chain transfer reaction will occur (the most feasible side reaction in this polymerization is the β -elimination). The transition state for β -H elimination is given in Chart 5, in which a β -agostic interaction is present that forces the polymerization chain either up or down directly into the ligand. The α -agostic interaction, which is present in the transition state for propagation, will force the polymer chain into direct interaction with ligand, slowing the propagation. However, this effect is relatively smaller than expected (compare the reaction period for **9** and **10** listed in Table 3). Thus, racemic and C_1 - and C_{2v} -symmetric complexes will favorably assume the structure to perform the propagation reaction rather than β -H elimination by the steric effect of the substituents lying at 3,4-positions on the Cp ring. Thus, the polymerization by the C_1 -symmetric complex afforded

Scheme 6

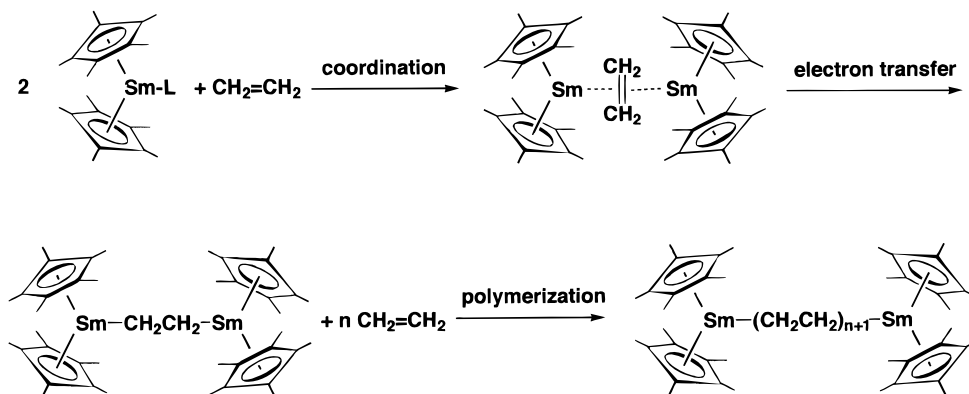


Table 3. Ethylene Polymerization by Divalent Sm Complexes^a

initiator	reacn period, min	activity, 10 ⁻⁴ g of PE/(mol h)	10 ⁻⁴ M _n	M _w /M _n
<i>rac</i> -tBu 7	1	6.18	11.6	1.43
	3	13.9	35.6	1.60
<i>rac</i> -tBuMe ₂ Si(THF=3) 8		no polymerization		
<i>rac</i> -tBuMe ₂ Si(THF=1) 8	5		13.1	3.54
	10		14.2	4.33
<i>C</i> ₁ -symmetric 9	15	1.57	100	1.60
	30	1.42	145	1.89
<i>meso</i> 10	5	14.6	1.94	3.29
	10	47.0	4.73	3.49
<i>C</i> _{2v} -symmetric(Ph ₂ Si)(THF=2) 11		no polymerization		
<i>C</i> _{2v} -symmetric(Ph ₂ Si)(THF=1) 11	5		16.0	1.84
	10		49.6	2.42
<i>C</i> _{2v} -symmetric[(SiOSi) ₂] 12	14 h	130 g of PE/(mol h)	42.9	3.04

^a Reaction conditions: temperature, 23 °C; initiator concentration, 1.0 mM; solvent, toluene; ethylene pressure, 1 atm.

Chart 4

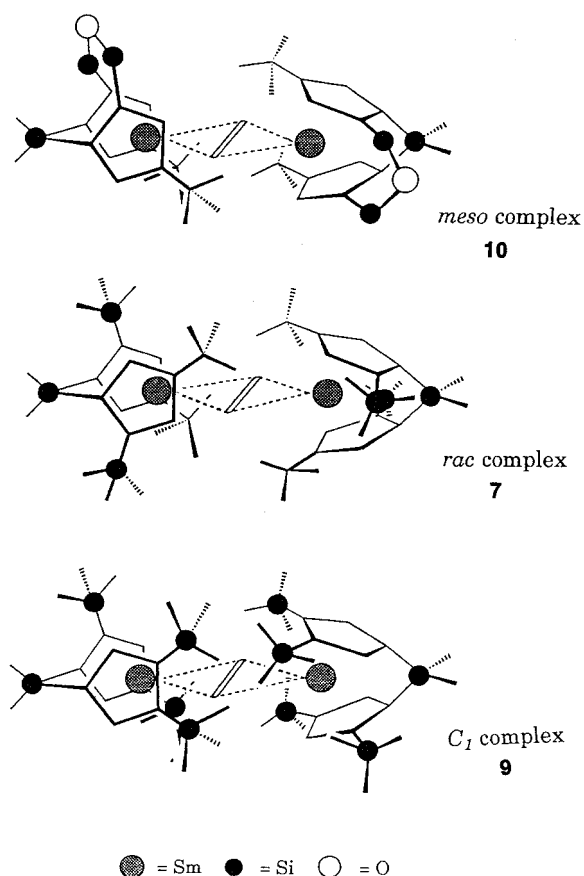
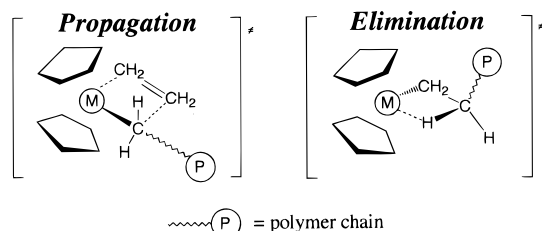


Chart 5



the highest molecular weight polyethylene. On the other hand, in the polymerization by a *meso* type complex with a large space around the metal center, β -elimination should occur more easily to result in the formation of rather low molecular weight polymers.

1-Olefin Polymerization. In contrast to the high activity of the divalent Sm complexes toward ethylene polymerization, only racemic complexes **7** and **8** are active for 1-olefin polymerization. Bercaw et al. reported that the trivalent racemic yttrium complex was active for stereoselective 1-olefin polymerization.⁶ Thus, the racemic structure seems to be essential to gain the activity. As mentioned in the former section, the characteristic feature of these racemic complexes lies in the deviation of the O(THF)–Sm–O(THF) plane from the equatorial plane defined by two Cp rings. The perturbation arising from the deviation may be related to the reactivity of 1-olefins toward these racemic complexes.

The result of the 1-olefin polymerization is summarized in Table 4. The polymerization proceeded in a highly stereoselective manner (isotactic) reflecting the *C*₂-symmetric structure. On the basis of ¹³C NMR analysis for the resulting poly(1-olefin)s, the isomer selectivities were higher than 95% (Figure 8).²² Thus, the polymerization mechanism for the present rare-earth-metal complexes is the same as that of group 4 metal Kaminsky type catalysts; i.e., *rac*-Et(Ind)₂MCl₂/methylalumoxane (M = Ti, Zr, Hf)^{23–26} and *rac*-Me₂Si(2-Me-4-naphthylindenyl)₂ZrCl₂/methylalumoxane²⁷ produce isotactic polypropylene. In these cases, propylene always inserts from the same site (the structure of the racemic complex given in Chart 4 is consistent with this expectation). More recently, *C*₁ type *threo*-Me₂C(3-tBu-C₅H₃)(3-tBu-C₉H₅)ZrCl₂ coupled with methylalumoxane was found to promote the isotactic polymerization of propylene.²⁸ The *meso* type complex **10** should afford the allylic complex as a result of β -H elimination (the color of the complex turned from purple to orange in the reaction with 1-hexene). In fact, both divalent (*C*₅-

(22) Asakura, T.; Demura, M.; Nishiyama, Y. *Macromolecules* **1994**, *24*, 2334.

(23) Ewen, J. A. *J. Am. Chem. Soc.* **1984**, *106*, 6355.

(24) Kaminsky, W.; Kulper, K.; Britzinger, H. H.; Wild, F. R. *Angew. Chem., Int. Ed. Engl.* **1985**, *24*, 507.

(25) Kaminsky, W.; Kulper, K.; Niedoba, S. *Makromol. Chem. Macromol. Symp.* **1986**, *3*, 377.

(26) Ewen, J. A.; Haspeslagh, L.; Atwood, J. L.; Zhang, H. *J. Am. Chem. Soc.* **1987**, *109*, 6544.

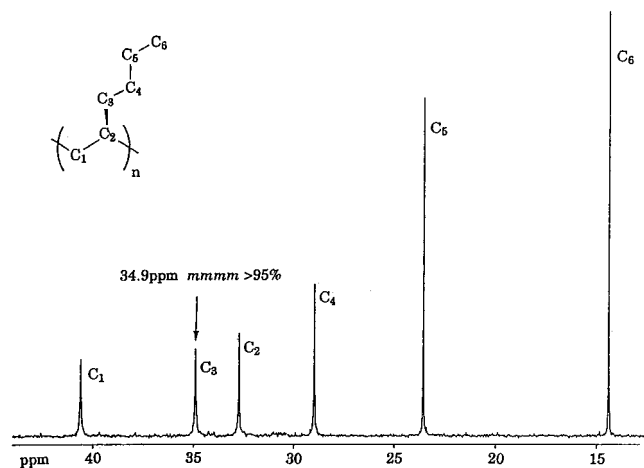
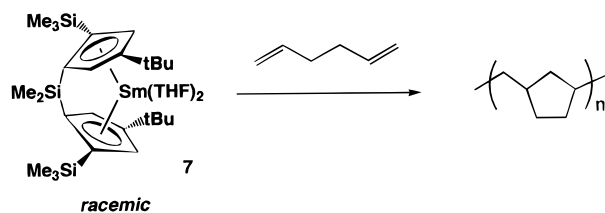
(27) Spaleck, W.; Kuber, F.; Winter, A.; Rohrmann, J.; Bachmann, B.; Antberg, M.; Dolle-Paulus, E. F. *Organometallics* **1994**, *13*, 945.

(28) Miyake, S.; Okumura, Y.; Inazawa, S. *Macromolecules* **1995**, *28*, 3074.

Table 4. 1-Olefin Polymerization by Divalent Sm Complexes^a

initiator	monomer	reacn period, h	activity, g of polymer/(mol h)	10 ⁻⁴ M _n	M _w /M _n
<i>rac</i> -tBu 7	1-pentene	12	161	1.06	1.48
		24	90	1.21	1.50
	1-hexene	12	138	0.83	1.55
		24	112	1.14	1.72
<i>rac</i> -tBuMe ₂ Si(THF=1) 8	1,5-hexadiene ^b	36	230	2.85	1.88
	1-pentene	48	98	0.59	1.70
	1-hexene	48	118	0.83	1.58

^a Reaction conditions: temperature, 23 °C; initiator, 0.01 mmol; solvent, 3.0 mL of toluene; monomer, 2.0 mL. ^b Initiator, 0.02 mmol.

**Figure 8.** ¹³C NMR spectrum of poly(1-pentene) obtained by use of complex **7**.**Scheme 7**

Me₅)₂Sm(THF)_x (*x* = 0, 2)²⁹ and trivalent [(C₅Me₅)₂Sm-(μ-H)]₂³⁰ complexes react with olefins to make only allyl products. During this procedure, the bite angle Cp(centroid)–Sm–Cp(centroid) should change freely from 116 to ca. 130°, because of the absence of a bridging group. In contrast to this observation, C₁ complex **9** and C_{2v} complexes **11** and **12** are completely inert toward 1-olefins due to steric reasons and the initial **9**, **11**, and **12** were recovered quantitatively.

In addition to the high activities of racemic complex **7** toward 1-pentene and 1-hexene, this complex is also active for the cyclopolymerization of 1,5-hexadiene, affording poly(methylene-1,3-cyclopentane) exclusively. The analysis of ¹³C NMR spectra of the resulting polymer shows that the selectivity of the ring-closing process is very low and the polymerization gave the methylene-1,3-cyclopentane structure within nearly a 1:1 *cis*:*trans* ratio (Scheme 7).³¹ High *trans* selectivity of poly(1,5-hexadiene) was already reported by Way-

mouth in the case of (C₅H₅)₂ZrCl₂, (C₅Me₅)₂ZrCl₂, and (*S,S*)-(EBETHI)ZrBINOL.^{32,33}

Experimental Section

General Considerations. All operations were performed under argon by using standard Schlenk techniques. Tetrahydrofuran and hexane were dried over Na/K alloy and distilled before use. Toluene used for polymerization was dried over Na/K alloy and thoroughly degassed by trap-to-trap distillation. Ethylene (Nakamura Oxygen Co.) was used without further purification. 1-Pentene, 1-hexene, and 1,5-hexadiene were dried over Na/K alloy and distilled. Me₃SiCl, Me₂SiCl₂, Ph₂SiCl₂, tBuMe₂SiCl, and ClMe₂SiOSiMe₂Cl were dried over CaH₂ for 1 week and used after distillation. The preparation of ligand **2** was already reported by Evans.¹¹ tBuCp-H was prepared by the reaction of tBuBr with CpNa, and Me₃SiCp-H was prepared by the reaction of Me₃SiCl with CpNa. (Me₃-Si)₂Cp-H was prepared by the reaction of Me₃SiCl with Me₃-SiCpNa. SmI₂ was prepared from Sm metal and diiodoethane in THF. ¹H NMR spectra were recorded on a Bruker AMX 400wb spectrometer (400.13 MHz), and chemical shifts were calibrated using benzene (δ 7.20 ppm). ¹³C NMR spectra were recorded on a JEOL JNM-LA 400 spectrometer (99.45 MHz), and chemical shifts were calibrated using the center peak of benzene (δ 128 ppm). Complexometric metal analyses were conducted by the method reported by Atwood and Evans.³⁴ M_n and M_w/M_n values of poly(1-pentene) and poly(1-hexene) were determined by gel permeation chromatography (GPC) on a Tosoh SC-8010 using TSKgel G2000, G3000, G4000, and G5000 columns in chloroform at 40 °C. M_n and M_w/M_n values of polyethylene were determined by GPC on a Waters 150C using a Shodex AT806MS column in 1,2,4-trichlorobenzene at 140 °C. M_n and M_w/M_n were calibrated from standard polystyrene.

Structure Solution and Refinement for Complexes 7, 8, 10, and 12. All the diffraction measurement were performed on a Rigaku AFC-5R diffractometer with graphite-monochromatized Mo Kα radiation. As the complexes are very air-sensitive, crystals were sealed in a thin-walled glass capillary tube under an argon atmosphere. The X-ray data were collected at room temperature using the ω–2θ scan technique to a maximum 2θ value of 55.0°. The data were corrected for conventional absorption, Lorentz, and polarization effects.

The crystal structures were solved by the heavy-atom method and were expanded by successive Fourier syntheses. The non-hydrogen atoms except for complex **7** (applied only for Sm, Si, O, and two C atoms in this case) were refined anisotropically by full-matrix least-squares methods, while the

(29) Evans, W. J.; Grate, W. J.; Choi, H. W.; Bloom, I.; Hunter, W. E.; Atwood, J. L. *J. Am. Chem. Soc.* **1985**, *107*, 941.

(30) Evans, W. J.; Bloom, I.; Hunter, W. E.; Atwood, J. L. *J. Am. Chem. Soc.* **1983**, *105*, 1401.

(31) Coates, G. W.; Waymouth, R. M. *J. Am. Chem. Soc.* **1993**, *115*, 91.

(32) Cavallo, L.; Guerra, G.; Corradini, P.; Resconi, L.; Waymouth, R. M. *Macromolecules* **1993**, *26*, 1260.

(33) Coates, G. W.; Waymouth, R. M. *J. Am. Chem. Soc.* **1993**, *115*, 91.

(34) Atwood, J. L.; Hunter, W. E.; Wayda, A. L.; Evans, W. J. *Inorg. Chem.* **1981**, *20*, 4115.

hydrogen atoms were fixed at their standard geometries and were not refined. All the calculations were performed by the use of the teXsan crystallographic software package (teXsan: Crystal Structure Analysis Package, Molecular Structure Corp. (1985 and 1992)).

Preparation of 7. To a stirred solution of **1** (3.01 g, 6.77 mmol) in THF (60 mL) was added *n*-BuLi (8.2 mL of 1.66 M solution in hexane, 13.5 mmol) at 0 °C. After the reaction mixture was stirred for 6 h at room temperature, *t*-BuOK (20 mL of 0.68 M solution in THF, 13.6 mmol) was added at that temperature. The resulting reaction mixture was refluxed for 12 h, and the solution was evaporated to dryness. The product was washed with hexane (30 mL \times 2), affording the dipotassium salt of **1** in 70% yield as a white powder. To 40 mL of THF were added at once at room temperature a THF suspension (80 mL) of the dipotassium salt of **1** (5.64 g, 10.8 mmol) and SmI₂ (80 mL of THF solution, 10.0 mmol). Then the reaction mixture was refluxed for 12 h and the solution was evaporated. Toluene (50 mL) was added to the residue, and insoluble solid was removed by centrifugation. After the solvent was removed in vacuo, the residue was extracted with THF (15 mL \times 2). Recrystallization from THF/hexane afforded **7** as purple crystals in 35% yield. ¹H NMR (400 MHz, C₆D₆): δ -12.82 (s, 2H, Cp H), -2.64 (s, 6H, Me₂Si), -1.05 (s, 8H, THF- β), 3.56 (s, 18H, SiMe₃), 4.05 (s, 8H, THF- α), 10.67 (s, 18H, tBu), 46.54 (s, 2H, Cp H). ¹³C NMR (99 MHz, C₆D₆): δ -5.01, 25.22, 29.83, 31.88, 46.05, 67.03. Anal. Calcd for SmC₃₄H₆₂Si₃O₂: Sm, 20.39. Found: Sm, 20.14.

Preparation of 8. To a stirred solution of **2** (4.70 g, 8.37 mmol) in THF (60 mL) was added *n*-BuLi (10.5 mL of 1.63 M solution in hexane, 17.0 mmol) dropwise at 0 °C. After the solution was stirred for 6 h at room temperature, *t*-BuOK (30 mL of 0.57 M solution in THF, 17.0 mmol) was added and the reaction mixture was refluxed for 12 h. A THF-hexane suspension of the dipotassium salt of **2** (8.37 mmol) was added to a THF solution (40 mL) of SmI₂ (90 mL, 8.0 mmol), and the reaction mixture was refluxed for 12 h. After removal of insoluble solid by centrifugation, the solvent was distilled out. A 50 mL portion of toluene was added to the residue, and insoluble solid was removed again by centrifugation. After the solution was evaporated, 30 mL of dimethoxyethane was added to the residue and the mixture was stirred for 12 h at room temperature. Removal of dimethoxyethane in vacuo followed by recrystallization of the residue from THF-hexane afforded **8** in 17% yield as purple crystals. ¹H NMR (400 MHz, C₆D₆): δ -8.50 (s, 2H, Cp H), -4.89 (s, 6H, tBuMe₂Si or Me₂Si), -2.27 (s, 6H, tBuMe₂Si or Me₂Si), -1.04 (s, 18H, SiMe₃), 0.77 (s, 8H, THF- β), 5.14 (s, 8H, THF- α), 8.90 (s, 18H, tBu), 13.45 (s, 6H, tBuMe₂Si or Me₂Si), 41.80 (s, 2H, Cp H). ¹³C NMR (99 MHz, C₆D₆): δ 11.60, 19.76, 20.93, 24.89, 27.46, 28.26, 29.83, 38.80. Anal. Calcd. for SmC₄₂H₈₂Si₅O₃: Sm, 16.24. Found: Sm, 16.54.

Preparation of 9. To a stirred solution of **3** (9.10 g, 19.1 mmol) in THF (80 mL) was added *n*-BuLi (23.4 mL of 1.63 M solution in hexane, 38.2 mmol) at 0 °C. The solution was stirred for 6 h at room temperature, and *t*-BuOK (30 mL of 1.33 M solution in THF, 40.0 mmol) was added. After the reaction mixture was refluxed for 12 h, the solution was evaporated to dryness. The product was washed with hexane (50 mL \times 2), affording the dipotassium salt of **3** in 94% yield as a white powder. To a THF suspension (120 mL) of the dipotassium salt of **3** (9.9 g, 17.9 mmol) was added SmI₂ (180 mL of THF solution, 17.0 mmol). The reaction mixture was refluxed for 12 h, and then the solvent was removed under vacuum. Toluene (50 mL) was added to the residue, and insoluble solid was removed by centrifugation. After the solution was evaporated, the residue was extracted with THF (15 mL \times 2). Recrystallization from THF/hexane afforded **9** as purple crystals in 28% yield. ¹H NMR (400 MHz, C₆D₆): δ -17.92 (s, 1H, Cp H), -6.16 (s, 3H, Me₂Si), -2.54 (s, 9H, SiMe₃), -1.58 (s, 8H, THF- β), 2.37 (s, 8H, THF- α), 4.12 (s, 3H,

Me₂Si), 6.92 (s, 9H, SiMe₃), 7.72 (s, 9H, SiMe₃), 17.85 (s, 9H, SiMe₃), 20.69 (s, 1H, Cp H), 23.83 (s, 1H, Cp H), 49.86 (s, 1H, Cp H). Anal. Calcd for SmC₃₂H₆₂Si₅O₂: Sm, 19.54. Found: Sm, 19.22.

Preparation of 10. To a stirred solution of **4** (3.39 g, 7.87 mmol) in THF (60 mL) was added *n*-BuLi (9.5 mL of 1.70 M solution in hexane, 15.7 mmol) at 0 °C. After the solution was stirred for 6 h at room temperature, *t*-BuOK (20 mL of 0.80 M solution in THF, 16.0 mmol) was added. The reaction mixture was refluxed for 12 h, and the solution was evaporated to dryness. The product was washed with hexane (50 mL \times 2) to afford the dipotassium salt of **4** in 96% yield as a white powder. A THF suspension (120 mL) of the dipotassium salt of **4** (3.82 g, 7.53 mmol) was added to SmI₂ (80 mL of THF solution, 7.40 mmol). The reaction mixture was refluxed for 12 h, and the solution was evaporated. Then, toluene (50 mL) was added to the residue and insoluble solid was removed by centrifugation. After the solvent was removed in vacuo, the residue was extracted with THF (15 mL \times 2). Recrystallization from THF/hexane afforded **10** as purple crystals in 66% yield. ¹H NMR (400 MHz, C₆D₆): δ -4.99 (s, 18H, tBu), -2.54 (s, 3H, Me₂Si), -1.09 (s, 6H, Me₂SiOSiMe₂), 3.19 (s, 8H, THF- β), 6.30 (s, 2H, Cp H), 10.51 (s, 8H, THF- α), 10.75 (s, 3H, Me₂-Si), 11.26 (s, 6H, Me₂SiOSiMe₂), 41.26 (s, 2H, Cp H). ¹³C NMR (99 MHz, C₆D₆): δ 4.63, 24.30, 28.90, 29.82, 30.95, 35.10, 42.80, 44.91. Anal. Calcd for SmC₃₂H₅₆Si₃O₃: Sm, 20.78. Found: Sm, 20.40.

Preparation of 11. To a stirred solution of **5** (4.75 g, 7.90 mmol) in THF (60 mL) was added *n*-BuLi (9.6 mL of 1.64 M solution in hexane, 15.8 mmol) dropwise at 0 °C. After the solution was stirred for 6 h at room temperature, *t*-BuOK (30 mL of 0.63 M solution in THF, 19.0 mmol) was added. The reaction mixture was refluxed for 36 h, and the solution was evaporated to dryness. The product was washed with hexane to afford dipotassium salt of **5** as white powder. A THF suspension (40 mL) of the dipotassium salt of **5** (7.90 mmol) was added to a THF solution of SmI₂ (60 mL, 3.46 mmol) at -78 °C, and the temperature of the reaction mixture was raised gradually to room temperature. After the reaction mixture was refluxed for 12 h, the solution was evaporated. Toluene (70 mL) was then added to the residue and insoluble solid was removed by centrifugation. Recrystallization of the toluene solution afforded **11** as purple crystals in 54% yield. ¹H NMR (400 MHz, C₆D₆): δ 29.41 (br s, 4H, Cp H), 14.10 (br s, 8H, THF- α), 8.83 (d, *J* = 6.5 Hz, 4H, Ph H [ortho]), 8.56 (t, *J* = 6.5 Hz, 4H, Ph H [meta]), 8.31 (t, *J* = 6.5 Hz, 2H, Ph H [para]), 2.15 (br s, 8H, THF- β), 0.22 (s, 36H, Me₃Si). Anal. Calcd for SmC₄₂H₆₆Si₅O₂: Sm, 16.82. Found: Sm, 16.13.

Preparation of 12. To a stirred solution of **6** (3.39 g, 6.71 mmol) in THF (45 mL) was added *n*-BuLi (9.8 mL of 1.64 M solution in hexane, 16.1 mmol) at 0 °C. After the solution was stirred for 5 h at ambient temperature, *t*-BuOK (20 mL of 1.18 M solution in THF, 35.4 mmol) was added. The reaction mixture was stirred for 12 h, and the solution was evaporated to dryness. The product was washed with hexane (80 mL), affording the dipotassium salt of **6** as a white powder. To a THF solution of SmI₂ (50 mL, 5.7 mmol) was added a THF suspension (50 mL) of the dipotassium salt of **6** (6.71 mmol) at room temperature. Then the reaction mixture was stirred for 12 h at room temperature and the solution was evaporated to dryness. At this point toluene (50 mL) was added to the residue and insoluble solid was removed by centrifugation. After the solvent was again removed under reduced pressure, recrystallization from THF/hexane afforded **12** as purple crystals in 23% yield. ¹H NMR (400 MHz, C₆D₆): δ -1.37 (s, 18H, tBu), 2.60 (s, 8H, THF- β), 3.10 (s, 12H, Me₂SiOSiMe₂), 6.18 (s, 12H, Me₂SiOSiMe₂), 6.70 (s, 4H, Cp H), 11.63 (s, 8H, THF- α). ¹³C NMR (99 MHz, C₆D₆): δ 13.08, 19.21, 23.30, 29.49, 43.55, 50.90. Anal. Calcd for SmC₃₄H₆₂Si₄O₄: Sm, 18.85. Found: Sm, 19.03.

Typical Procedure for Ethylene Polymerization. A solution of an initiator (0.02 mmol) in 20 mL of toluene was exposed to 1 atm of ethylene. The reaction mixture was stirred for an appropriate period at room temperature. The polymerization was stopped by the addition of methanol. The resulting polyethylene was washed with methanol twice and dried in vacuo.

Typical Procedure for 1-Olefin Polymerization. To a toluene solution (3 mL) of an initiator (0.02 mmol) was added 2 mL of a monomer at room temperature. The reaction mixture was stirred for an appropriate period at room temperature. The polymerization was stopped by addition of methanol. The resulting polymer was washed with methanol twice and dried in vacuo.

Acknowledgment. This work was supported by a Grant-in-Aid for Scientific Research on Priority Areas (No. 283, "Innovative Synthetic Reactions") from Monbusho.

Supporting Information Available: Text and figures detailing the preparation methods for ligands **1–6** and tables of atomic coordinates and equivalent isotropic displacement parameters, bond distances, bond angles, and hydrogen atom coordinates for complexes **7**, **8**, **10**, and **12** (62 pages). Ordering information is given on any current masthead page.

OM971099U